International Journal of Pharmaceutics: X 4 (2022) 100125

Contents lists available at ScienceDirect

International Journal of Pharmaceutics: X

journal homepage: www.sciencedirect.com/journal/international-journal-of-pharmaceutics-x

Modelling intramuscular drug fate *in vitro* with tissue-relevant biomimetic hydrogels

Adam McCartan [a], Julia Mackay [a], David Curran [b], Randall J Mrsny [a,*]

[a] Department of Pharmacy & Pharmacology, University of Bath, Bath BA2 7AY, Avon, UK
[b] CMC Analytical, GlaxoSmithKline, Collegeville, PA 19426, USA

ARTICLE INFO

Keywords:
Intramuscular
Biomimetic
Hydrogels
In vitro
Drug fate
Modelling

ABSTRACT

Parenteral administrations are a mainstay of clinical drug delivery. Intramuscular (IM) injections deposit drug directly into skeletal muscle bellies, providing rapid systemic uptake due to the highly vascularized nature of this site. The potential to inject particulate or non-aqueous materials have also made IM injections useful for long-acting formulations. These attributes have supported a plethora of medicines being approved for IM administration. Despite these many approvals across multiple pharmaceutical categories, mechanisms that control drug release from the injection site, and thus its pharmacokinetic properties, remain poorly understood. Several pre-clinical *in vivo* animals have been used to model IM drug fate in patients, but these approaches have not consistently predicted clinical outcomes. This lack of a predictive *in vivo* model and no standardized *in vitro* tools have limited the options of pharmaceutical scientists to rationally design formulations for IM delivery. Here, we describe a novel, tractable *in vitro* model informed by dominant extracellular matrix (ECM) components present at the IM injection site. Three charge variants of green florescent protein (GFP) and the impact of three common formulation components were examined in an initial test of this *in vitro* model. A strongly positively charged GFP was restricted in its release from hydrogels composed of ECM components type I collagen and hyaluronic acid compared to standard and strongly negatively charged GFP. Introduction of commonly used buffers (histidine or acetate) or the non-ionic surfactant polysorbate 20 altered the release properties of these GFP variants in a manner that was dependent upon ECM element composition. In sum, this *S*imulator of *I*ntra*M*uscular *I*njections, termed SIMI, demonstrated distinct release profiles of a protein biopharmaceutical surrogate that could be exploited to interrogate the impact of formulation components to expedite novel drug development and reduce current dependence on potentially non-predictive pre-clinical *in vivo* models.

1. Introduction

The intramuscular (IM) administration route is a common parenteral alternative to the oral delivery of pharmaceuticals that show poor physiochemical stability in, or limited uptake from, the gastrointestinal tract. The IM injection deposits formulations directly into skeletal muscle bellies, where diffusion through fascial planes of the skeletal muscle organ precedes uptake into the systemic vasculature or lymphatics (Newton et al., 1992; Ogston-Tuck, 2014). In general, drugs delivered by IM injection are formulated for immediate absorption using rapidly diffusing aqueous formulations that takes advantage of the highly vascularized nature of this tissue (*e.g.* epinephrine) or as long-acting injectables (LAIs) which gradually release drug in a controlled manner over weeks or months (*e.g.* haloperidol decanoate) (Gu et al., 1999; Whyte and Parker, 2016). Despite the large number of drugs approved by regulators for IM injection, there is limited knowledge of how these drugs interact with the IM environment, *i.e.*, drug fate (McCartan et al., 2021). At present there are no standardized *in vitro* tools available to researchers to investigate IM drug fate for the generation of descriptive pharmacokinetic (PK) data; the development of IM-injected drugs relies heavily on pre-clinical *in vivo* models, but these *in vivo* models fail to consistently predict human clinical outcomes (McCartan et al., 2021). Acellular *in vitro* modelling offers the potential for powerful, in-depth investigations that can address specific drug fate hypotheses in tractable experimental formats (McCartan et al., 2021).

IM-injected drug formulations distribute along the fascial planes

Abbreviations: Collagen type 1, Col1; Interstitial fluid, ISF; Hyaluronic acid, HA; Simulator of intramuscular injections, SIMI.

* Corresponding author.
E-mail address: rjm37@bath.ac.uk (R.J. Mrsny).

https://doi.org/10.1016/j.ijpx.2022.100125
Received 20 May 2022; Received in revised form 22 July 2022; Accepted 3 August 2022
Available online 13 August 2022

established by the endomysium (space between individual muscle fibres) and perimysium (encapsulating individual muscle fibres into fascicles) within a skeletal muscle belly (Darville et al., 2016; Evertz et al., 2016; Groseclose and Castellino, 2019; Kalicharan et al., 2016; Kameni Tcheudji et al., 2016; Probst et al., 2016). The endomysium and perimysium compartments contain lymphatic and vascular capillaries, nerve fibres, and a variety of cells including adipocytes, fibroblasts, and macrophages, but is dominated by an extracellular matrix (ECM) composed of large macromolecules that organize and stabilize skeletal muscle fibres. A predominantly serum-derived interstitial fluid (ISF) is assumed to flow through the endomysium and perimysium. As very little of an IM-injected drug formulation enters individual muscle fibres, events of interaction with and dissemination through ECM elements of the endomysium and perimysium would dominate their fate following administration. Whilst the exact components and concentrations of ISF are still debated, ECM elements of the endomysium and perimysium are well documented with fibrillar collagen type 1 (Col1) being the dominant protein component (Gordon and Hahn, 2010; Loukas et al., 2008; Purslow, 2002) and hyaluronic acid (HA) being the predominant non-protein element (Fraser et al., 1997; Piehl-Aulin et al., 1991).

Previous efforts to model the IM injection environment have employed hydrogels composed of such ECM elements, including thiol-modified HA and glycosaminoglycans, and even decellularised/reconstituted animal skeletal muscle ECM (Narayanan et al., 2021; Prestwich, 2008; Wassenaar et al., 2015). Indeed, "micro-tissues" and whole excised muscle tissue have previously been described as *in vitro* and *ex vivo* IM-injection models, respectively (Afshar et al., 2020; Napaporn et al., 2000). Such models, however, are technically and financially challenging to use in large scale assays over long time scales. As such, acellular *in vitro* methodologies are typically favoured for their advantages in cost-effectiveness, user-friendliness, and tractable experimental design. For such approaches to be of value to pharmaceutical scientists, a tractable model that allowed for the rational addition or exclusion of specific ECM and formulation components is required. Such a model should include components that emulate critical elements of the IM injection site that might control drug binding and a means to monitor drug release from that environment over time under physiologically relevant conditions (McCartan et al., 2021).

Here, we have explored an initial design for a novel *in vitro* tool to model IM-specific drug fate, termed the *S*imulator of *I*ntra*M*uscular *I*njections (abbreviated to SIMI). Col1 and HA were used in hydrogel formats to model potential interactions between the predominant protein and non-protein ECM materials that would be experienced by formulation components following their IM injection. These ECM-like hydrogels were contained within a semi-porous non-specific cuvette, which in turn was suspended in an ISF-mimic buffer solution to represent the infinite sink of the body following uptake into vascular or lymphatic capillaries. Initial tests using this format were performed using green fluorescent proteins (GFP) having three distinct global charge profiles alongside clinically relevant excipients (Lawrence et al., 2007; Pramanick et al., 2013). These GFP variants were selected as a surrogate drug to provide a means to readily visualise the injection bolus formed within the hydrogel and to simultaneously examine the impact of drug charge on drug-ECM binding events. Diffusion of these GFP variants from the ECM-hydrogels into the infinite sink compartment were monitored for rapid (first several hours) and extended release (release at 24 h) to examine the impact of biopharmaceutical properties and formulation components on drug fate. This prototype system showed that release of a material from a hydrogel mimicking the IM injection site was affected by ECM composition and that this release could be monitored by measuring drug entry into the surrounding ISF-mimic solution. By following this diffusion over time, descriptive PK profiles of an injected drug and/or formulation materials could be obtained. These studies support the SIMI model as a potential *in vitro* model to screen IM-focused formulations for impact of ECM components on drug fate following injection.

2. Materials and methods

2.1. Hydrogel generation

Bovine Col1 solution (Sigma C2124-50ML) and HA (Sigma 53,747-10G) were used in hydrogel preparations. 0.01 M HCl, prepared in double-distilled water ($_{dd}H_2O$), was used to dilute Col1 solutions that were neutralized with 0.1 M NaOH prepared in $_{dd}H_2O$. 10× concentrated PBS stocks were prepared with NaCl (1.37 M), KCl (27 mM), $Na_2HPO_4 \bullet 7H_2O$ (95 mM), KH_2PO_4 (18 mM) and sodium azide (30 mM) in $_{dd}H_2O$, adjusted to pH 7.4 with HCl. Separate 10× PBS stocks were prepared including 5 mg/mL HA, mixed for at least 48 h to ensure complete solubilisation and homogenous mixing. 5 mL volume hydrogels were generated by diluting Col1 in 0.01 M HCl, and combining with 0.1 M NaOH and 10× concentrated PBS plus/minus 5 mg/mL HA in a ratio of 8:1:1, respectively, and incubated at 37 °C for at least 1 h. Final concentration of PBS in the hydrogel therefore equalled 1× PBS. For rheological assessment, 1.5 mL volume hydrogels were used containing 3.2 mg/mL Col1 and 0.5 mg/mL HA, or 3.2 mg/mL Col1 only. For the *in vitro* SIMI model, 5 mL volume hydrogels had final concentrations of 1 mg/mL Col1 and 0.5 mg/mL HA, or 1 mg/mL Col1 only.

2.2. Rheology

Rheological assessment of hydrogels was conducted with a Discovery HR-3 Hybrid Rheometer and Trios software (TA Instruments, DE, USA). A 40 mm Peltier steel plate was used in a parallel plate setup with a gap of 500 μm. 1.5 mL hydrogels were used for investigations. All experiments were conducted at plate temperatures of 37 °C. Each assessment was composed of three individual analyses. Oscillation frequency analysis was conducted at 0.5% strain, 0.1–100 rad/s. Oscillation amplitude analysis was conducted using an angular frequency of 6.28319 rad/s, with a strain range of 0.01–50%. Flow analysis was conducted over an increasing shear rate of 0.01 to 100 1/s with a 5 s equilibration time and 30s averaging time.

2.3. ISF-mimic buffer

The ISF-mimic buffer was composed of NaCl (109.5 mM), KCl (5.4 mM), $MgCL_2.6H_2O$ (0.4 mM), $CaCl_2.2H_2O$ (1.8 mM), HEPES (20 mM) and sodium azide (3.1 mM) in $_{dd}H_2O$. The pH was set at 7.4 by titration with 0.5 M HCl and 0.5 M NaOH as required. For dilution of GFP stocks and preparation of "formulations", the same solution, excluding HEPES, was used.

2.4. In vitro tool setup

140 mL of ISF buffer was decanted into a 150 mL beaker with a stirrer bar and warmed to

37 °C on a heated stirrer (200 rpm). The pH was then adjusted to 7.4. The 5 mL hydrogels were transferred into semi-permeable cuvettes of 6 mL volume (Pion #10900–0001, USA) and suspended with polystyrene floats in the warmed ISF buffer for at least 15 min prior to commencing experiments.

2.5. Expression of GFP, GFP + 36 and GFP-30

GFP and "supercharged" GFP proteins were prepared from plasmids containing the genes for GFP with a net −7 charge (GFP-std), a net +36 charge (GFP-pos), and a net −30 charge that were kindly provided by Dr. David Liu (Lawrence et al., 2007). Amino acid sequences for GFP-std, GFP-pos, and GFP-neg along with calculated values for molecular weight and isoelectric point (pI) are provided in Supplementary Data. All three GFP variants were expressed in Shuffle T7 Express competent *E. coli* (NEB) grown at 37 °C in Terrific broth supplemented with glycerol and containing kanamycin to an extinction of 0.6 at 600 nm. The

temperature was reduced to 16 °C and isopropyl β-D-thiogalactopyranoside (IPTG) was added to a final concentration of 0.5 mM. Growth was continued at 16 °C overnight before cells were harvested by centrifugation, resuspended in 20 mM Tris pH 8, 1 M NaCl, 20 mM imidazole and lysed by sonication. Lysates were centrifuged and supernatant filtered through a 0.45-μm filter. Protein purification was performed using a 5-mL HisTrap™ column (GE Healthcare) connected to an AKTA FLPC. Bound proteins were eluted using a 0.05–1 M imidazole gradient and further purified using a Superdex® 200 gel filtration column equilibrated with PBS. Protein purity was assessed by SDS-PAGE and protein concentration was assessed using A280 prior to storage at −80 °C.

2.6. Formulation excipients and in vitro study

GFP, L-histidine (Fisher BP383–100), sodium acetate (Sigma S2889), and polysorbate 20 (Sigma P1379) were diluted with HEPES-free ISF buffer. The formulations were: GFP-only (2 mg/mL), GFP-L-histidine (2 mg/mL and 25 μM, respectively), GFP-acetate (2 mg/mL and 25 μM, respectively) and GFP-PS20 (2 mg/mL and 30 mg/mL, respectively). GFP-only formulations were pH 7.4, while GFP formulations with L-histidine, acetate, and PS20 were pH 6. Injections (200 μL) were made into the centre of hydrogels using an Eppendorf repeater E3x (Eppendorf #4987000029) with an Eppendorf 1 mL advanced Combitip advanced (Eppendorf #0030089430) and a 21 G microlance needle, at the injection rate of 10 s/mL. 300 μL of ISF buffer was sampled immediately before injection (*i.e.*, $T = 0$), then at 10-, 20-, and 30-min post-injection. Thereafter ISF buffer was sampled at 1-, 2-, 3-, 4-, 5-, and 24-h post-injection. ISF buffer samples were stored in sterile 1.5 mL Eppendorf tubes at 4 °C until analyzed.

2.7. GFP quantification

For GFP quantification, 100 μL ISF buffer duplicates were added to black plastic 96 well Nunclon Delta plates (Thermo #137101). The samples were measured for fluorescence intensity with a FLUOstar Omega plate reader using Omega control and data analysis software (BMG Labtech). The excitation wavelength was set at 480 nm, and the emission wavelength set at 520 nm. Data was transferred to Microsoft Excel for data analysis.

3. Results

3.1. Organization of SIMI, an in vitro simulator of the intramuscular injection site

Plastic cuvettes (6 mL volume) with two opposing sides containing windows of dialysis membrane were filled with 5 mL hydrogels prepared from dominant ECM components present at the IM injection site: Col1 and Col1/HA. The hydrogel-filled cuvette was placed in a 140 mL stirred volume of media designed to emulate interstitial fluid (ISF), mimicking the infinite sink of the body, that could be used to measure release of molecules injected into the hydrogel over time (Fig. 1). By preparing hydrogels of different ECM elements, this system provided a tractable model to assess potential interactions between specific ECM elements and drug formulation components at an IM injection site prior to their absorption into blood or lymph. Thus, release characteristics of injected materials would be affected by specific and/or non-specific binding interactions with these ECM elements as well as biophysical properties of the hydrogel that affected diffusion. While the intent of the SIMI model was to emulate the human IM injection site, bovine Col1 was used in these initial studies rather than the human protein. BLASTp analysis using UniProt sequences for Col1 alpha-1 and alpha-2 chains (Supplementary Data Table 1) verified high sequence homology between bovine Col1 and human Col1, making this system realistic for modelling the human IM injection site. Amino acid homology of the bovine Col1 alpha-1 and alpha-2 chains was >90% identical to human Col1 alpha chains (Supplementary Data Table 2), indicating satisfactory similarity for use of bovine Col1 in the initial, proof-of-concept model.

3.2. Rheological characterisation reveals similar hydrogel viscoelastic properties

Rheological assessment initially studied the relationship between the loss modulus (G") and storage modulus (G') of hydrogel formats containing 3.2 mg/mL Col1 and 0.5 mg/mL HA, or 3.2 mg/mL Col1 alone across an increasing frequency range, known as a frequency sweep (Fig. 2A). Sterile hydrogels of 1.5 mL volume used in these studies were consistently colourless and translucent. Tan(δ) values obtained using the Discovery HR-3 rheometer described the ratio between G" and G', *i.e.*, dissipated energy and stored energy within the hydrogel matrix. Across the range of 0.1 to 100 rad/s frequency, the tan(δ) values decreased greatest between 0.1 and 10 rad/s for both Col1/HA and Col1 hydrogel formats. Past the 10 rad/s frequency point, the tan(δ) values remained stable. Results from both hydrogel formats overlapped across the entire frequency range studied, indicating similar elastic properties of both

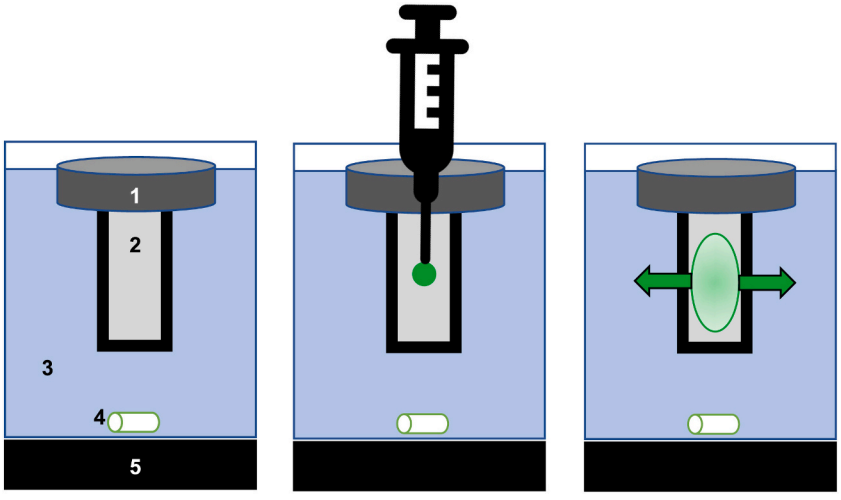

Fig. 1. The *S*imulator of *I*ntra*M*uscular *I*njection (SIMI) *in vitro* modelling tool.
(A) A polystyrene float (1) suspended a 5 mL hydrogel contained within a semi-porous cuvette (2), suspended in interstitial fluid-mimicking buffer (37 °C, pH 7.4) (3). The whole system was stirred (4) on a heated stirring plate (5). (B) Materials were directly injected (vertically) into the hydrogel at a 90° angle to form a bolus. (C) Over time, injected material distributes through the hydrogel matrix, before releasing through the non-specific membranes into the buffer system. The buffer can then be sampled for quantifying drug at discreet time points.

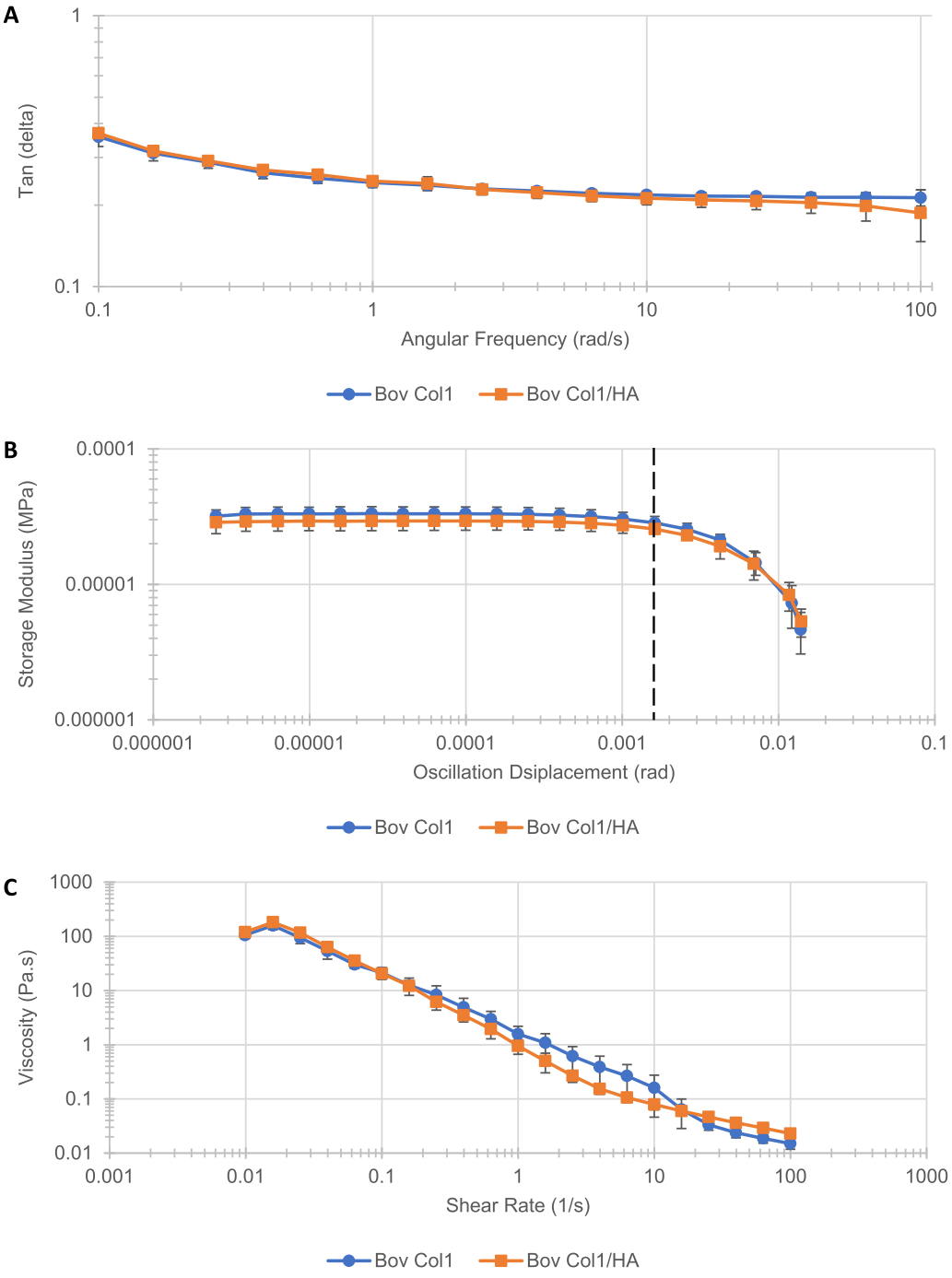

Fig. 2. Rheological characterisation of 3.2 mg/mL bovine Col1 (circles) and 3.2 mg/mL bovine Col1, 0.5 mg/mL HA (squares) hydrogel formats by (A) frequency sweep, (B) amplitude sweep and (C) flow sweep analysis. (A) Frequency analysis determined the ratio of loss and storage moduli across increasing angular frequency. (B) Amplitude analysis determined the linear visco-elastic range of the hydrogels (dashed vertical line indicates visco-elastic limit of both hydrogel formats). (C) Flow analysis determined "flowing" properties of the hydrogels under increasing stress. Mean +/− standard deviation. All series, $n = 3$.

Col1/HA and Col1 hydrogel formats. Amplitude sweeps were used to measure hydrogel viscoelasticity, where energy applied to the hydrogels was increased by enlarging the oscillation amplitude (Fig. 2B). Here, the Col1/HA format was less elastic than the Col1 alone format when considering G'. This could be because the extended chains of HA, extending throughout the Col1 network, reduced the amount of free space available for elastic deformation of Col1. The linear viscoelastic limit, however, was equal for both hydrogel formats at approximately 0.0016 rad (marked by a vertical dashed line; Fig. 2B). This indicated similar viscoelastic behaviour between the two hydrogel formats. Lastly, flow sweep assays characterized how these hydrogels "flowed" under increasing stress (Fig. 2C). The data indicated that both hydrogel formats possess the non-Newtonian characteristic of shear thinning: as the degree of stress applied to the hydrogels increased, viscosity decreased. The Col1/HA format hydrogel exhibited lower viscosity than the Col1 alone format under shear rates of 0.1–10 1/s. At all other measured shear rate points, the data from both hydrogel formats again overlapped. Overall, these findings indicated how Col1/HA and Col1 hydrogels were similar in the rheological parameters studied and could be compared to each other in further experiments.

3.3. *Protein charge affects injection site release characteristics*

Green fluorescent protein (GFP) was selected as a surrogate to monitor distribution of an injected drug and to examine the impact of biomolecule charge on its release from the injection site compartment of the SIMI model. GFP, composed of 248 amino acids with a molecular mass of ~28 kDa, was prepared as three distinct genetic variants that

had an overall charge of −7 (GFP-std), supercharged negative at −30 (GFP-neg), or supercharged positive at +36 (GFP-pos). These GFPs were prepared in non-buffered ISF-mimic solution (adjusted to pH 7.4) prior to injection into hydrogels prepared from 1 mg/mL Col1/0.5 mg/mL HA or 1 mg/mL Col1 alone. The extent of GFP-std and GFP-neg released from Col1/HA and Col1 hydrogel formats were comparable at 24 h, while the total amount of GFP-pos released over this time was much less compared to GFP-std or GFP-neg release (Fig. 3A). Data obtained over the first 5 h showed distinct release profiles for all three GFPs (Fig. 3B). The initial 10-min release profile of all GFP variants may be due to a portion of injected material that exceeded the extent of immediate hydrogel matrix interactions for the SIMI model format, with the subsequent release profile defining the release based upon hydrogel matrix interactions. Whilst currently undetermined, this may be a relevant *in vivo* event occurring post-IM injection. Release of GFP-pos reached a maximum after approximately 20–30 min for both Col1/HA and Col1 hydrogel formats. GFP-std release was comparable for both Col1/HA and Col1 hydrogel formats over the entire 24 h period, and similar to GFP-neg release from the Col1/HA hydrogel over 24 h (Fig. 3B). There was a general trend of increased release rates for GFP-pos and GFP-neg in the Col1 hydrogel format when compared to the Col1/HA format (Fig. 3B).

3.4. Formulation components can affect injection site release characteristics

3.4.1. L-Histidine

L-Histidine is a physiological buffer commonly used to formulate proteins in the pH range of 5–7, utilizing the pKa 6.1 of its imidazole moiety (Osterberg and Wadsten, 1999). We examined the potential for this amino acid to affect the release of GFP variants from the hydrogels of pH 7.4 (maintained by phosphate of PBS), where L-histidine would be positively charged. Release of the three GFP variants formulated in 25 μM L-histidine in buffer-free ISF solution (the formulation pH was adjusted to pH 6) were studied over 24 h after their injection into the 1 mg/mL Col1/0.5 mg/mL HA or 1 mg/mL Col1 alone hydrogels (Fig. 4A).

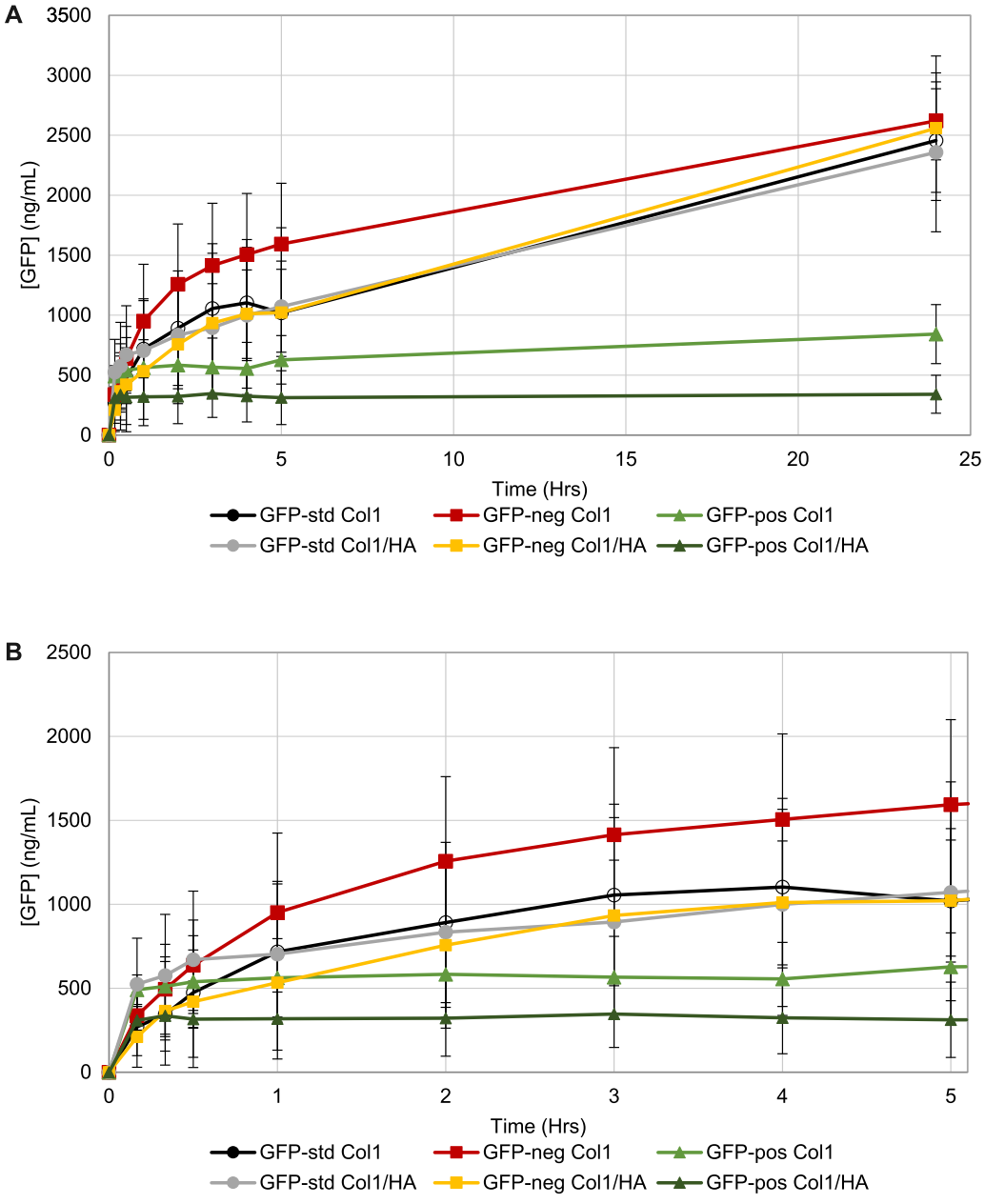

Fig. 3. Green fluorescent protein (GFP) in its standard form (GFP-std; circles), supercharged negative (GFP-neg; squares) or supercharged positive (GFP-pos; triangles) show impact of overall charge on release rates following injection into hydrogels composed of 1 mg/mL Col1/0.5 mg/mL HA or 1 mg/mL Col1. (A) Release over 24 h. (B) Magnified release over the first 5 h. Mean +/− standard deviation. GFP-std Col1, $n = 3$. GFP-std Col1/HA, $n = 4$. GFP-neg all series, $n = 3$. GFP-pos all series, $n = 4$. (For interpretation of the references to colour in this figure legend, the reader is referred to the web version of this article.)

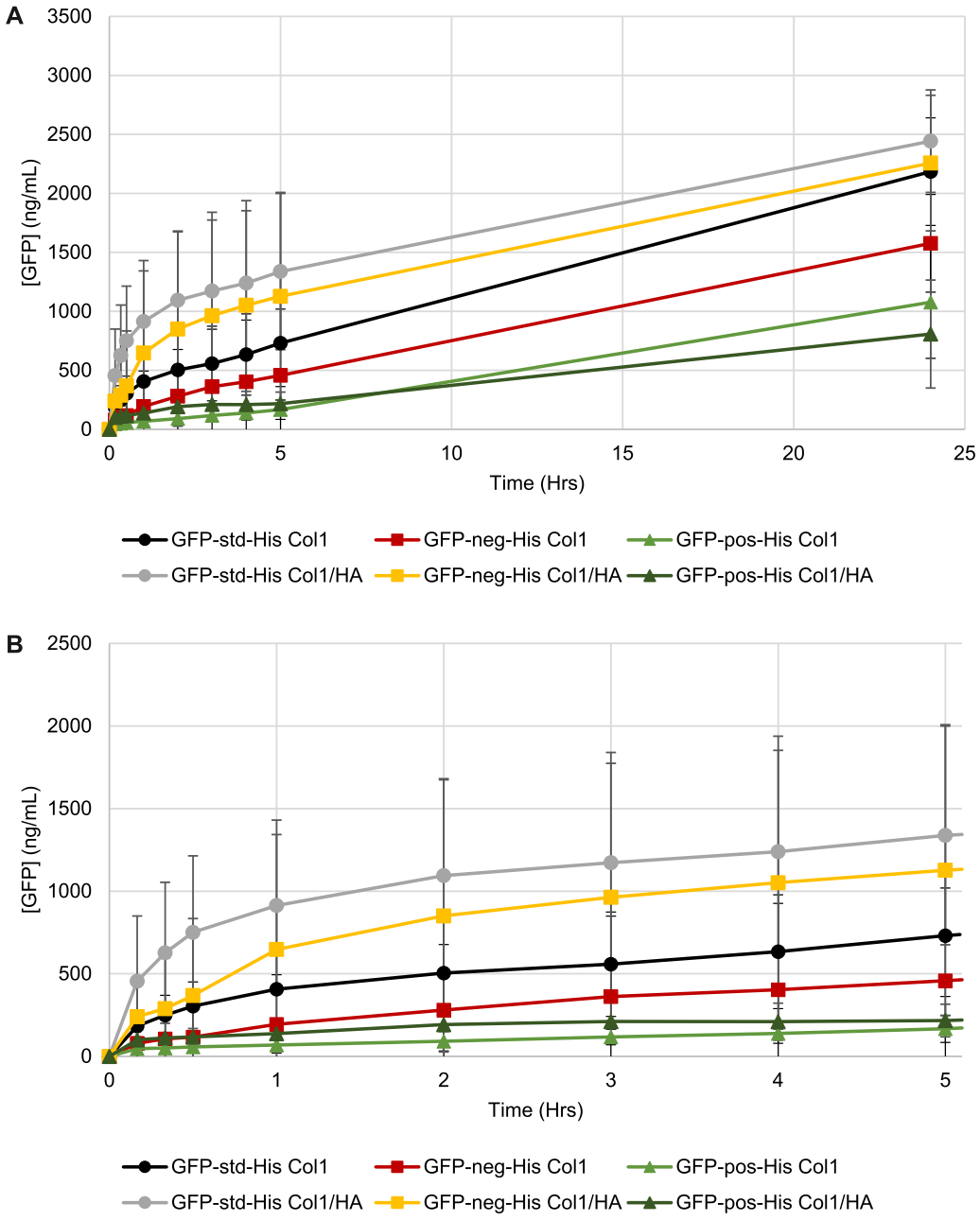

Fig. 4. Effect of 25 μM L-histidine (His) on the release of green fluorescent protein (GFP) in its standard form (GFP-std; circles), supercharged negative (GFP-neg; squares), or supercharged positive (GFP-pos; triangles) following injection into hydrogels composed of 1 mg/mL Col1/0.5 mg/mL HA or 1 mg/mL Col1. (A) Release over 24 h. (B) Magnified release data over the first 5 h. Mean +/− standard deviation. GFP-std Col1, $n = 4$. GFP-std Col1/HA, $n = 6$. GFP-neg Col1, $n = 4$. GFP-neg Col1/HA, $n = 6$. GFP-pos all series, $n = 4$. (For interpretation of the references to colour in this figure legend, the reader is referred to the web version of this article.)

After 24 h, GFP-std release from Col1/HA and Col1 hydrogels as well as GFP-neg from the Col1/HA hydrogel were comparable, with the total amounts released being similar for these proteins formulated without L-histidine (Fig. 3A). GFP-neg release from the Col1 only hydrogel was reduced in comparison to the other GFP test formats (Fig. 4A), and from that observed when GFP-neg was injected into Col1 alone hydrogels without L-histidine (Fig. 3A). The total amount of GFP-pos formulated in L-histidine released from Col1/ HA or Col1 hydrogel was further reduced compared to GFP-std and GFP-neg (Fig. 4A) but released to a greater degree than when this protein was formulated without L-histidine (Fig. 3A).

Differences in GFP release from these hydrogel formats was apparent after only 10 min when injected in L-histidine formulations (Fig. 4B). Initial GFP-pos release from either Col1/HA or Col1 hydrogels was reduced compared to profiles obtained without L-histidine (Fig. 3B), with greater retention of GFP-pos in these hydrogels over the first 5 h (Fig. 4B). GFP-neg formulated with L-histidine released steadily from the Col1 hydrogel but was initially retained like GFP-pos in both hydrogel formats (Fig. 4B). Further, GFP-neg released more readily from Col1/HA than Col1 hydrogels (Fig. 4B), where non-formulated GFP-neg released more readily from Col1 only hydrogels (Fig. 3B). In the case of GFP-std, release profiles over the first 5 h without added L-histidine were similar (Fig. 3B), but release from Col1/HA was faster than from Col1 alone when formulated with L-histidine (Fig. 4B).

3.4.2. Acetate

Acetate is a physiological buffer commonly used to formulate proteins in the pH range 2.5–7, utilizing the pKa 4.75 of acetic acid (Pramanick et al., 2013). We examined the potential for this weak acid to affect the release of GFP variants from the hydrogels of pH 7.4 (maintained by phosphate of PBS) where it would be negatively charged. Release of GFPs formulated in 25 μM sodium acetate in buffer-free ISF (the formulation pH was adjusted to pH 6) were studied over 24 h after their injection into 1 mg/mL Col1/0.5 mg/mL HA or 1 mg/mL Col1 only

hydrogels (Fig. 5A), with these outcomes being compared to release data obtained without added acetate (Fig. 3A). At 24 h, only one of the acetate-formulated systems showed limited release: GFP-pos injected into Col1/HA hydrogels. GFP-pos with acetate injected into Col1 only hydrogels released to a similar degree as GFP-neg from Col1 only gels after 24 h (Fig. 5A). All other formats demonstrated protein release outcomes at 24 h in the range expected based on non-formulated GFP data (Figs. 4A, 3A). Despite these similar ultimate release outcomes after 24 h, differences in release profiles were observed during the first 5 h after injection (Fig. 5B). Acetate-formulated GFP-std and GFP-neg showed fast, comparable release following injection into Col1/HA hydrogels. By comparison, these release profiles were diminished over the first 5 h after injection into Col1 alone hydrogels (Fig. 5B).

3.4.3. *Polysorbate 20*

Polysorbate 20 (PS20) is a non-ionic surfactant (formed by sorbitan ethoxylation prior to adding lauric acid) widely used in protein biopharmaceutical formulations as an excipient to stabilize emulsions and suspensions as well as minimize their binding to surfaces during purification and storage (Ionova and Wilson, 2020). Release of GFPs formulated in 30 mg/mL PS20 at pH 6 in non-buffered ISF-mimic solution were studied over 24 h after their injection into 1 mg/mL Col1/0.5 mg/mL HA or 1 mg/mL Col1 alone hydrogels (Fig. 6A) and compared to non-formulated GFP data (Fig. 3A). PS20 accelerated release of GFP-neg from Col1/HA hydrogels in the first 5 h (Fig. 6A). After 24 h, the extent of PS20-formulated GFP-neg release from Col1/HA hydrogels was the greatest degree of GFP-neg release in the studies performed (Figs. 3, 4, 5, 6). GFP-neg release from Col1, and GFP-std release from Col1/HA and Col1 hydrogels, was reduced compared to the moderate level of release observed in initial GFP studies (Figs. 6A, 3A). PS20 had little impact on the amount of GFP-pos released from Col1/HA or Col1 hydrogels, consistent with the release profiles of these highly cationic macromolecules in the formulation scenarios described above. PS20-formulated GFP-neg and GFP-std injected into Col1

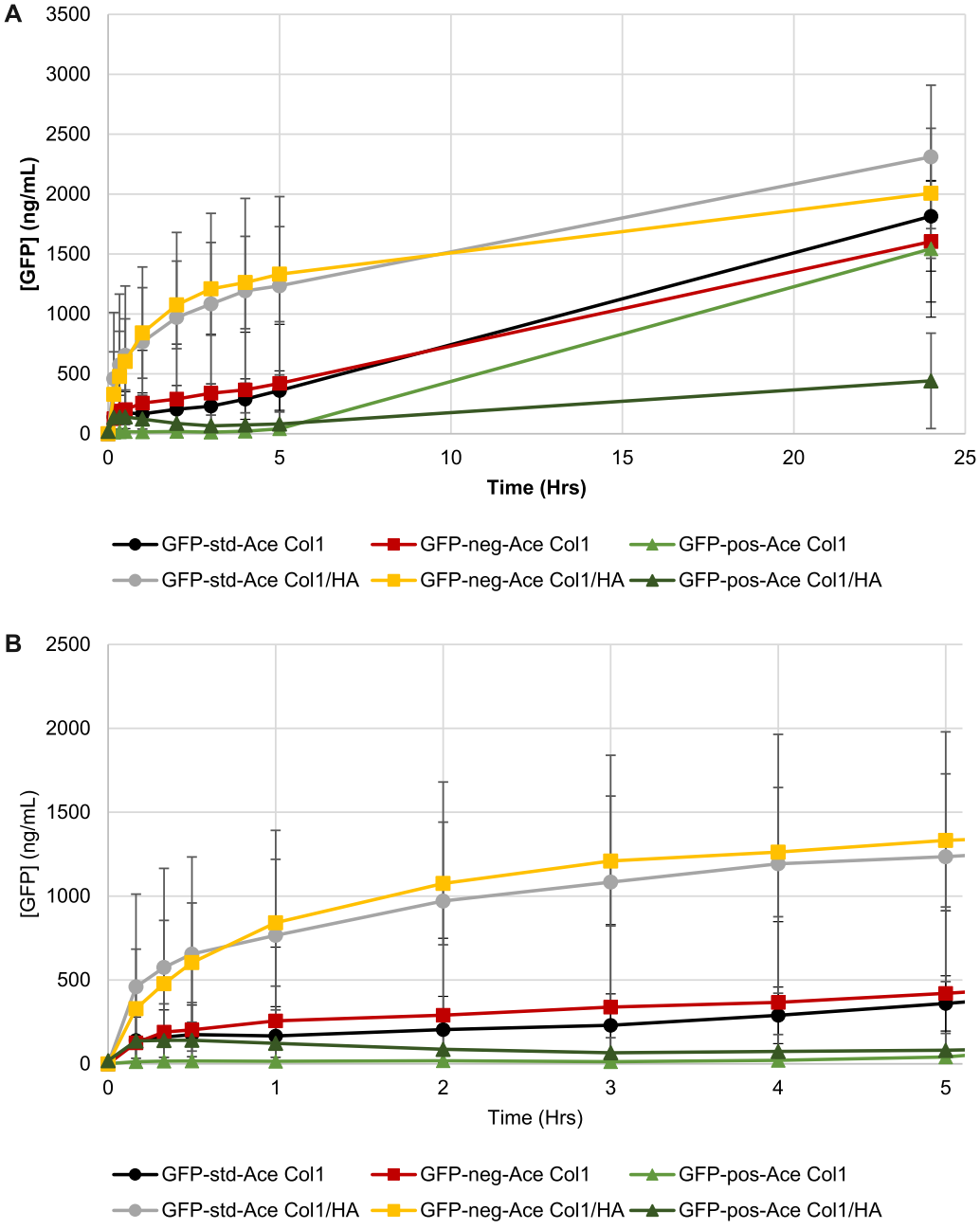

Fig. 5. Effect of 25 μM sodium acetate (Ace) on the release of green fluorescent protein (GFP) in its standard form (GFP-std; circles), supercharged negative (GFP-neg; squares), or supercharged positive (GFP-pos; triangles) following injection into hydrogels composed of 1 mg/mL Col1/0.5 mg/mL HA or 1 mg/mL Col1. (A) Release over 24 h. (B) Magnified release data over the first 5 h. Mean +/− standard deviation. All series, $n = 4$. (For interpretation of the references to colour in this figure legend, the reader is referred to the web version of this article.)

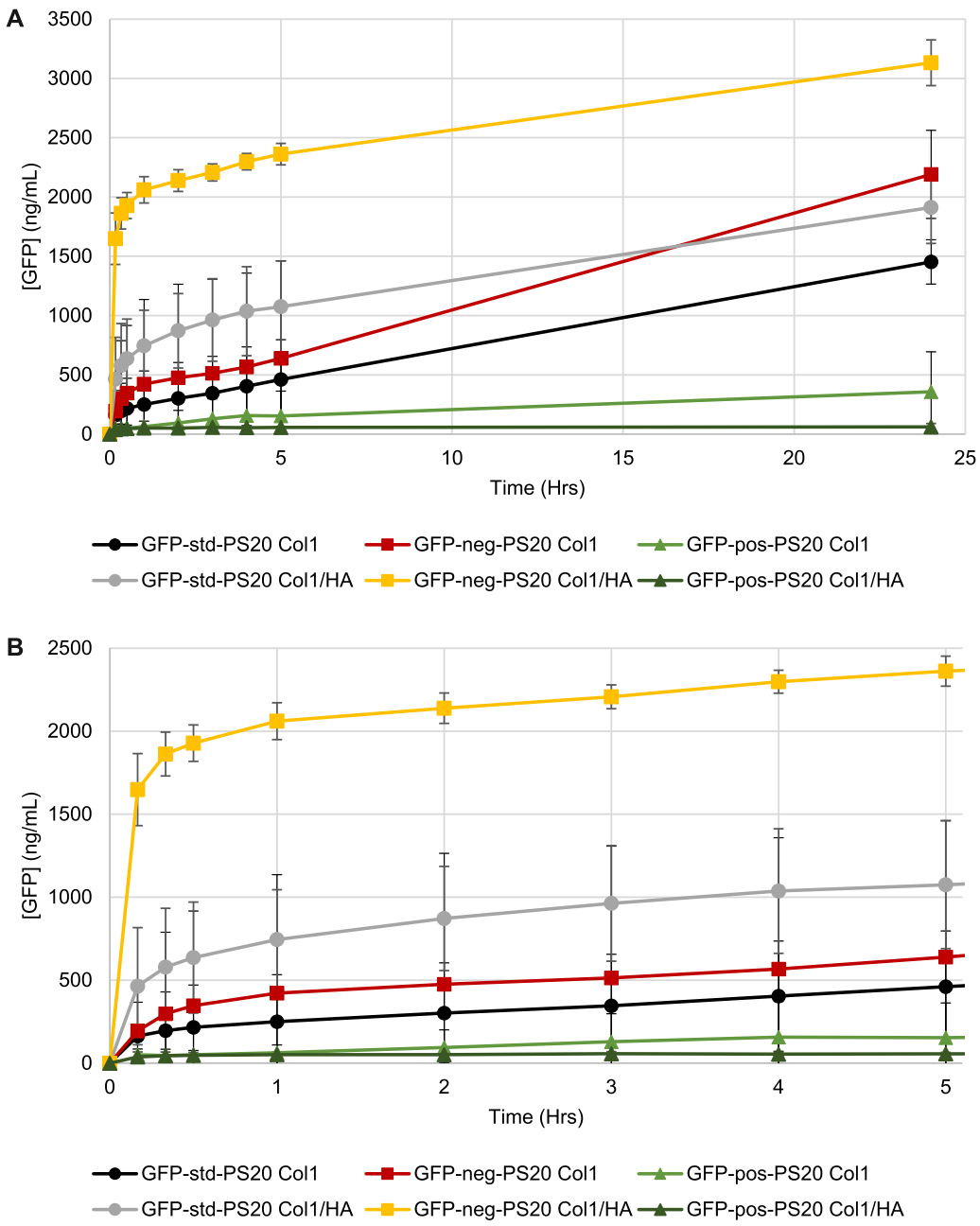

Fig. 6. Effect of 30 mg/mL polysorbate 20 (PS20) on the release of green fluorescent protein (GFP) in its standard form (GFP-std; circles), supercharged negative (GFP-neg; squares), or supercharged positive (GFP-pos; triangles) following injection into hydrogels composed of 1 mg/mL Col1/0.5 mg/mL HA or 1 mg/mL Col1. (A) Release over 24 h. (B) Magnified release data over the first 5 h. Mean +/− standard deviation. All series $n = 4$. (For interpretation of the references to colour in this figure legend, the reader is referred to the web version of this article.)

hydrogels were not released as readily as that observed following injection into Col1/HA hydrogels (Fig. 6B).

3.5. *Excipients affected GFP release based on protein charge and hydrogel composition*

The physiological buffers L-histidine and acetate, and the non-ionic surfactant PS20, are commonly used in formulating injected protein therapeutics. These formulations, adjusted to pH 6, are not intended for long-term buffering of pharmaceuticals post-IM injection. This initial pH discrepancy would be swiftly resolved to physiological pH 7.4 *in vivo*, and is hypothesised to occur in the SIMI hydrogel (buffered to pH 7.4 with pospohate). This pH transition, as an event in itself, would likely be trivial in its impact on GFP release. These excipients were found to affect the release properties of three differently charged variants of GFP, dependent on the ECM components in the hydrogel. To compare the relative impact of these agents more readily, 24 h GFP release outcomes were plotted as the fraction of release over time (Fig. 7). The extent of impact produced by addition of these protein formulation components was expressed as the absolute difference to that observed for these three GFP variants lacking one of these additives.

With GFP-std, L-histidine or acetate demonstrated minimal impact on GFP-std release from the Col1/HA hydrogels (Fig. 7A). However, the surfactant PS20 did reduce GFP-std release from 81% to 67% at 24 h (Fig. 7A). This was a lesser impact than that observed in the Col1 hydrogel, reducing total GFP-std release from approximately 86% to 50% after 24 h (Fig. 7B). In the Col1 only hydrogel, inclusion of L-histidine or acetate reduced GFP-std release to 76% and 63%, respectively (Fig. 7B). Initial GFP-std release was consistent between all formulations in the Col1/HA format (Fig. 7A), whilst distinct release profiles were observed when using Col1 only hydrogels (Fig. 7B).

GFP-neg release over 24 h was 89% in Col1/HA hydrogels (Fig. 7C), comparable to 92% release observed in Col1 only hydrogels (Fig. 7D). PS20 caused a large initial increase in GFP-neg release within 5 h, that

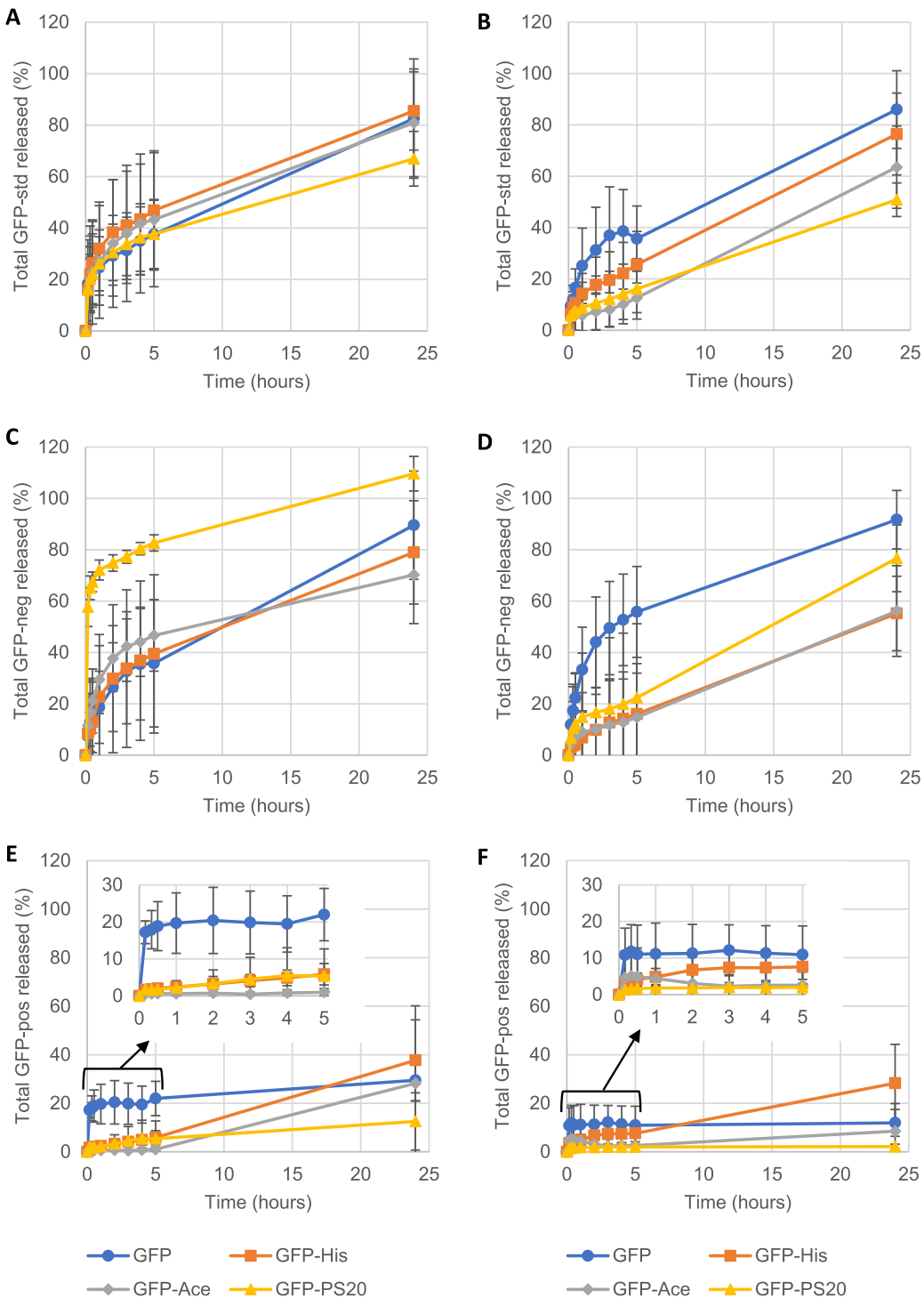

Fig. 7. Total release of (A, B) native GFP, (C, D) supercharged negative GFP and (E, F) supercharged positive GFP was compared to formulations containing 25 μM L-histidine (His; squares), 25 μM sodium acetate (Ace; diamonds) or 30 mg/mL polysorbate 20 (PS20; triangles) over 24 h. Hydrogels were composed of (A, C & E) 1 mg/mL Col1/0.5 mg/mL HA or (B, D & F) 1 mg/mL Col1. (E & F) Inset magnifies initial release of GFP-pos. Mean +/− standard deviation. Data is reformulated from Figs. 3, 4, 5, 6 with corresponding *n* numbers.

resulted in 100% GFP release at 24 h (Fig. 7C). This exceeded total release of GFP-neg when co-formulated with L-histidine (79%) or acetate (70%) in Col1/HA hydrogels (Fig. 7C). In the Col1 alone hydrogel, inclusion of L-histidine or acetate caused the greatest decrease in total GFP-neg release, 56% for both excipients, whilst PS20 had a lesser impact, reducing total GFP-neg release to 77% (Fig. 7D).

GFP-pos release from the Col1/HA hydrogel was 30%, more than double the 12% observed in the Col1 format (Fig. 7E, F). In the Col1/HA hydrogel, the addition of acetate or PS20 reduced total GFP release after 24 h to 28% and 13% respectively, whilst L-histidine increased total GFP-pos release to 38% (Fig. 7E). In the Col1 hydrogel, GFP-pos release was further reduced by inclusion of acetate (9%) or PS20 (2%) while L-histidine increased total GFP-pos release to 28% after 24 h (Fig. 7F).

4. Discussion

The *in vitro* tool we describe here, referred to as the SIMI, was designed to test an initial *in vitro* system concept to model IM injected material distribution and release *in vivo*. IM injections result in the distribution of drug formulations within the endomysium and perimysium of striated muscle. While a variety of cell types are found in these locations (fibroblasts, endothelial cells, *etc.*), the SIMI does not

incorporate cells and thus is not amenable to testing formations such as RNA-based vaccines, that involve cell-based outcomes. Instead, the SIMI is intended to examine the fate of IM-injected therapeutics where the fate of these materials would be potentially affected by interactions with acellular inter-fascial ECM components that dominate these regions. This ECM is primarily composed of Col1, imparting strength and a framework for interactions with other ECM elements. HA is one of most prominent of these other elements, functioning as a biological lubricant to retain water and minimize friction between fascial layers during dynamic muscle movement (McCartan et al., 2021). Based upon their relative abundance, these ECM components were identified for this initial modelling of the IM injection site. For these studies, we established a Col1 hydrogel format at physiological pH (7.4) and temperature (37 °C) that was by itself, and in combination with HA, translucent and colourless. These features allow for direct visual and spectroscopic assessment of events within the compartment following introduction of a test formulation. Our proof-of-concept format used 5 mL volumes of these two hydrogel matrices as injection compartment that could accept 200 μL volumes of a test formulation in an arrangement that allowed detection of released materials into an ISF-mimic buffer that modelled the infinite sink of the body.

The hydrogel matrix and buffer designs used here were simplistic; both the IM fascial layers and ISF contain many components not represented in the current SIMI design, such as soluble proteins in the ISF (which may affect the release of poorly water-soluble drugs *in vivo*). Buffering elements used in the current SIMI format were also non-physiological: phosphate (presented in PBS) in the hydrogel, and HEPES in the ISF-mimic solution. These buffers were selected for their properties and ease of use in generating a pilot tool. PBS has been frequently applied in Col1-based hydrogel design and shown to be chemically stable in a pH 7.4 solution. HEPES is also chemically stable in aqueous settings, with a pKa of 7.5 that was ideal to maintain pH 7.4 in the ISF-mimic buffer. Both PBS and HEPES offered simplified alternatives to a more complex, bio-relevant buffer which can be difficult to maintain at a desired pH over extended periods (Kinnunen et al., 2015). Further research should replace PBS and HEPES with bicarbonate buffering components to reflect this foundational element of the ISF *in vivo*. This will, however, require technologies to continuously monitor pH and administer CO_2 gas accordingly to maintain pH 7.4 in the SIMI environments. However, there is no guarantee that specific IM environment components, such as bicarbonate, will impact drug fate outcomes. Candidate components for inclusion in the SIMI compartments must therefore be evaluated accordingly.

The two hydrogel formats we describe here were assessed for their rheological properties. Both hydrogel formats were indeed similar in viscoelasticity and non-Newtonian behaviour; shear thinning is well-documented in biomaterial hydrogels and has been exploited in injectable-hydrogel drug-delivery strategies (Chen et al., 2017; Loebel et al., 2017). However, the 3.2 mg/mL Col1 content used in rheological analysis was too high for injection modelling in the SIMI, as injected materials were immediately ejected along the needle bore. This frustrated efforts to form an injection bolus, which was desired in the SIMI to reflect *in vivo* observations of injected pharmaceuticals forming bolus deposits (Darville et al., 2016). Reducing Col1 content to 1 mg/mL produced stable hydrogels that were sufficiently malleable for bolus formation and dissemination through the hydrogel matrix following injection of a formulation. By sampling the ISF-mimic buffer over 24 h, we established the release profiles of charged GFP variants, in several formulations, from boluses formed in the hydrogel environment. The hydrogel matrix of Col1 and HA may influence movement of molecules by steric hindrance; bulkier drugs, such as macromolecules, may be retained longer at the injection site while small molecules could more freely move through the Col1/HA network. Of these components, Col1 is noted to be positively charged at physiological pH (Andrade et al., 2004; Li and Katz, 1976), whilst HA is negatively charged (Travis et al., 2001). These distinctly charged components may influence diffusion of strongly charged molecules and macromolecules through electrostatic interactions, further retaining molecules in the hydrogel matrix after injection or encouraging their diffusion from the matrix and into the infinite sink compartment.

In the SIMI, we observed that GFP-std and GFP-neg generally displayed negative exponential curve release profiles. These indicate a decay of GFP presence at the injection site as GFP diffuses through the hydrogel matrix (with no distinct inhibitory interactions) before releasing into the ISF-mimic buffer. These non-formulated GFPs were prepared for injection with no buffering agents; there are no other potential interactions occurring other than GFP with the hydrogel and ISF-mimic systems. However, GFP-pos generally released slowly from the injection site, independent of hydrogel composition, suggesting specific interactions with the Col1 matrix. In this regard, several proteins, including von Willebrand factor and various growth factors, specifically bind Col1 *in vivo* (Cauble et al., 2017; Liu et al., 2003; Romijn et al., 2003).

Clear differences were observed in the release profiles of GFP over the 24-h window of analysis that were assumed to describe interaction parameters between the distinct physical properties of the GFP variants and Col1 or Col1/HA matrices. Interestingly, we observed a similar initial release of all non-formulated GFP variants at 10 min post-injection that did not reflect the extent of release after 24 h. The reason for this phenomenon is unclear but could be due to pressure introduced into the hydrogel by the injection process. This added force may have been sufficient to transiently overcome the interactive forces between the injected GFP variant and the hydrogel components that ultimately defined the extent of release observed after 24 h. As materials then "settle" post-injection, the injection-pressure force should diminish. Interactions with the hydrogel matrix would dominate and reflect interactions that control diffusion away from the bolus site. Interestingly, the extent of this initial "burst" observed at 10 min post-injection was dramatically altered for studies that examined additions of L-histidine, acetate, or PS20. Here, the release at 10 min post-injection directly correlated with the extent of release after 24 h, suggesting that the presence of these additives affected the extent of initial interactions during this "burst" between the GFP variant and the Col1 or Col1/HA hydrogels in a way that overcame the added pressure associated with the injection event. This impact of excipient presence on this initial "burst" and 24 h release was further investigated by exploiting the tractable nature of the SIMI.

By using Col1/HA and Col1 only hydrogel formats, we examined the individual roles Col1 and HA in determining drug fate outcomes for these GFP variants. Absence of HA in hydrogels did not affect non-formulated GFP-std release, but reduced release when formulated with L-histidine, acetate or PS20 (Figs. 7A 7B). Yet, non-formulated GFP-pos release over 24 h was doubled in the presence of HA (Fig. 7E, F). Such data indicated how HA can affect IM drug fate outcomes, dependent on drug characteristics and distinct from the effects of Col1. Excipients, too, appeared to alter this interaction dynamic between GFP and the hydrogel matrix, dependent on GFP charge and/or hydrogel composition. For example, L-histidine increased GFP-pos release from both hydrogel formats, while acetate or PS20 reduced release. Indeed, acetate generally reduced diffusion of all GFP variants in both hydrogel formats. Whilst the mechanisms of these observations are unclear, a histidine-rich glycoprotein can block Col1 interactions with endothelial cells (Roche et al., 2015) while sodium eugenol acetate (derived from sodium acetate) inhibited Col1-dependent platelet aggregation *in vitro* (Chen et al., 1996). Hypothetically, L-histidine and acetate may directly interact with Col1 networks, reducing interactions with GFP. Distinct in function from L-histidine and acetate, surfactant PS20's ability to stabilize proteins at interfaces may have led to altered protein-hydrogel matrix interactions. Whilst PS20 generally reduced the release of all GFP variants in all hydrogels, such stabilisation may be significant for strongly negative macromolecules: GFP-neg formulated with PS20 in Col1/HA hydrogels exhibited expedited diffusion away from the

injection site (Fig. 7C). Yet, PS20 decreased release of GFP-neg compared to non-formulated GFP-neg in Col1 only hydrogels (Fig. 7D), indicating HA-surfactant interplay. Presently, the mechanisms relating to such outcomes with PS20 (and indeed L-histidine and acetate) are not clear. However, the SIMI was designed to explore such examples of drug fate outcomes in a fully tractable manner, to establish how excipients modify drug behaviour post-IM administrations. As such, with further development and application of the SIMI, such mechanisms could be elucidated.

In formulation design, the long-term stability of a drug is essential to allow storage of the product before administration. As such, formulations may use low concentrations (*i.e.*, 25 μM) of buffering excipients, as used in this study, for maintaining non-physiological pH (*i.e.*, pH 6). However, such designs are not intended for buffering drug formulations *in vivo* post-administration. These non-physiological pH conditions will likely rapidly transition to physiological pH post-injection, and are modelled here in the SIMI (*i.e.*, μM quantities of formulation excipient, *versus* overwhelming mM quantities of phosphate in the hydrogel). While the initial change in pH of the environment is likely to be inconsequential, the results of this change may have a role in drug fate. Transitions to physiological pH may alter the overall charge state of excipients with respect to their pKa values, thereby possibly influencing potential interactions with the local IM environment.

While this initial version of the SIMI model has begun to uncover the role of drug, excipient, and injection site properties and their interplay in drug fate outcomes, it must be acknowledged that further work is crucial in establishing its true value in modelling human IM conditions. Evaluation and validation of the SIMI by *in vitro – in vivo* correlations (IVIVC), and indeed mathematical modelling of drug PK, have yet to be undertaken. While IVIVC data could be explored to establish *e.g.*, equivalence of the SIMI to standard *in vivo* models such as rats, it is the ability to model human PK outcomes that is paramount for SIMI model applications. Such validation can indeed be conducted using published human PK data from the PharmaPendium database (Elsevier), which contains data for a wide range of IM-approved pharmaceuticals, from small molecules to proteins, in an array of quick or slow releasing formulations. Examples of drugs with such PK data available have been tabulated (McCartan et al., 2021).

The GFP variants used in these studies provided a surrogate set of molecules to emulate protein biopharmaceuticals with distinct charge properties. In this initial SIMI model format, the potential for charge interactions between biopharmaceuticals and ECM components were examined and found to dominate release characteristics from the hydrogel matrices composed of Col1 and HA. Furthermore, our with these GFP variants demonstrated how formulation excipient choices might impact IM drug fate outcomes. Further development of SIMI technologies would permit further exploration of potential events affecting drug fate *in vivo*, such as whether individual excipients directly interacting with IM site components, such as Col1. This kind of descriptive data, informing behavioural trends of injected materials, may be useful to inform rational drug formulation design for IM administration.

5. Conclusions

IM drug fate is an area of limited knowledge, despite the increasing application of IM pharmaceuticals in the clinic. Here, we have described an initial effort to establish a tractable *in vitro* tool for investigating parameters of drug fate after IM administrations. From the data presented and discussed here, the SIMI appears to allow discrimination of distinct biopharmaceutical properties and can evaluate specific formulation excipients that may impact drug performance at the IM site in a tractable manner. Using the model, we have begun to identify pharmaceutical and formulation properties that can affect drug fate and to determine how specific ECM components of the IM injection site can likewise impact drug fate. Such an approach could be useful in formulation screening studies to predict the likely performance of a pharmaceutical formulation to expedite research efforts by reducing dependence on costly, time-consuming *in vivo* experiments that may not actually be productive of outcomes in humans. Thus, after obtaining these initial proof-of-concept outcomes, efforts to use human ECM components and use a more physiologically relevant ISF composition are being contemplated for a next generation SIMI model.

Funding sources

Adam McCartan is a recipient of a GSK/EPSRC co-funded studentship (EP/P510403/1).

Research data

All data supporting this study is openly available from the University of Bath Research Data Archive (https://doi.org/10.15125/BATH-01146).

Declaration of Competing Interest

The authors declare the following financial interests/personal relationships which may be considered as potential competing interests:

Adam McCartan reports financial support was provided by Engineering and Physical Sciences Research Council. Adam McCartan reports financial support was provided by GSK.

Appendix A. Supplementary data

Supplementary data to this article can be found online at https://doi.org/10.1016/j.ijpx.2022.100125.

References

Afshar, M.E., Abraha, H.Y., Bakooshli, M.A., Davoudi, S., Thavandiran, N., Tung, K., Ahn, H., Ginsberg, H.J., Zandstra, P.W., Gilbert, P.M., 2020. A 96-well culture platform enables longitudinal analyses of engineered human skeletal muscle microtissue strength. Sci. Rep. 10, 6918.

Andrade, Â.L., Ferreira, J.M.F., Domingues, R.Z., 2004. Zeta potential measurement in bioactive collagen. Mater. Res. 7, 631–634.

Cauble, M., Yang, P., Baumann, U., Gebauer, J.M., Orr, B.G., Duong, L.T., Banaszak Holl, M.M., 2017. Microstructure dependent binding of pigment epithelium derived factor (PEDF) to type I collagen fibrils. J. Struct. Biol. 199, 132–139.

Chen, S.J., Wang, M.H., Chen, I.J., 1996. Antiplatelet and calcium inhibitory properties of eugenol and sodium eugenol acetate. Gen. Pharmacol. 27, 629–633.

Chen, M.H., Wang, L.L., Chung, J.J., Kim, Y.H., Atluri, P., Burdick, J.A., 2017. Methods to assess shear-thinning hydrogels for application as injectable biomaterials. ACS Biomater. Sci. Eng. 3, 3146–3160.

Darville, N., van Heerden, M., Erkens, T., De Jonghe, S., Vynckier, A., De Meulder, M., Vermeulen, A., Sterkens, P., Annaert, P., Van den Mooter, G., 2016. Modeling the time course of the tissue responses to intramuscular long-acting paliperidone palmitate nano−/microcrystals and polystyrene microspheres in the rat. Toxicol. Pathol. 44, 189–210.

Evertz, L.Q., Greising, S.M., Morrow, D.A., Sieck, G.C., Kaufman, K.R., 2016. Analysis of fluid movement in skeletal muscle using fluorescent microspheres. Muscle Nerve 54, 444–450.

Fraser, J.R.E., Laurent, T.C., Laurent, U.B.G., 1997. Hyaluronan: its nature, distribution, functions and turnover. J. Intern. Med. 242, 27–33.

Gordon, M.K., Hahn, R.A., 2010. Collagens. Cell Tissue Res. 339, 247–257.

Groseclose, M.R., Castellino, S., 2019. Intramuscular and subcutaneous drug depot characterization of a long-acting cabotegravir nanoformulation by MALDI IMS. Int. J. Mass Spectrom. 437, 92–98.

Gu, X., Simons, F.E., Simons, K.J., 1999. Epinephrine absorption after different routes of administration in an animal model. Biopharm. Drug Dispos. 20, 401–405.

Ionova, Y., Wilson, L., 2020. Biologic excipients: Importance of clinical awareness of inactive ingredients. PLoS One 15, e0235076.

Kalicharan, R.W., Baron, P., Oussoren, C., Bartels, L.W., Vromans, H., 2016. Spatial distribution of oil depots monitored in human muscle using MRI. Int. J. Pharm. 505, 52–60.

Kameni Tcheudji, J., Cannet, C., Gerard, C., Curdy, C., Beckmann, N., 2016. Long-term distribution of biodegradable microparticles in rat muscle quantified noninvasively by MRI. Magn. Reson. Med. 75, 1736–1742.

Kinnunen, H.M., Sharma, V., Contreras-Rojas, L.R., Yu, Y., Alleman, C., Sreedhara, A., Fischer, S., Khawli, L., Yohe, S.T., Bumbaca, D., Patapoff, T.W., Daugherty, A.L., Mrsny, R.J., 2015. A novel in vitro method to model the fate of subcutaneously

administered biopharmaceuticals and associated formulation components. J. Control. Release 214, 94–102.
Lawrence, M.S., Phillips, K.J., Liu, D.R., 2007. Supercharging proteins can impart unusual resilience. J. Am. Chem. Soc. 129, 10110–10112.
Li, S.T., Katz, E.P., 1976. An electrostatic model for collagen fibrils. The interaction of reconstituted collagen with Ca++, Na+, and Cl. Biopolymers 15, 1439–1460.
Liu, B., Weinzimer, S.A., Gibson, T.B., Mascarenhas, D., Cohen, P., 2003. Type Ialpha collagen is an IGFBP-3 binding protein. Growth Hormon. IGF Res. 13, 89–97.
Loebel, C., Rodell, C.B., Chen, M.H., Burdick, J.A., 2017. Shear-thinning and self-healing hydrogels as injectable therapeutics and for 3D-printing. Nat. Protoc. 12, 1521–1541.
Loukas, M., Shoja, M.M., Thurston, T., Jones, V.L., Linganna, S., Tubbs, R.S., 2008. Anatomy and biomechanics of the vertebral aponeurosis part of the posterior layer of the thoracolumbar fascia. Surg. Radiol. Anat. 30, 125–129.
McCartan, A.J.S., Curran, D.W., Mrsny, R.J., 2021. Evaluating parameters affecting drug fate at the intramuscular injection site. J. Control. Release 336, 322–335.
Napaporn, J., Thomas, M., Svetic, K.A., Shahrokh, Z., Brazeau, G.A., 2000. Assessment of the myotoxicity of pharmaceutical buffers using an in vitro muscle model: effect of pH, capacity, tonicity, and buffer type. Pharm. Dev. Technol. 5, 123–130.
Narayanan, N., Lengemann, P., Kim, K.H., Kuang, L., Sobreira, T., Hedrick, V., Aryal, U. K., Kuang, S., Deng, M., 2021. Harnessing nerve-muscle cell interactions for biomaterials-based skeletal muscle regeneration. J. Biomed. Mater. Res. A 109, 289–299.
Newton, M., Newton, D.W., Fudin, J., 1992. Reviewing the "big three" injection routes. Nursing 22, 34–41.
Ogston-Tuck, S., 2014. Intramuscular injection technique: an evidence-based approach. Nurs. Stand. 29, 52–59.
Osterberg, T., Wadsten, T., 1999. Physical state of L-histidine after freeze-drying and long-term storage. Eur. J. Pharm. Sci. 8, 301–308.
Piehl-Aulin, K., Laurent, C., Engström-Laurent, A., Hellström, S., Henriksson, J., 1991. Hyaluronan in human skeletal muscle of lower extremity: concentration, distribution, and effect of exercise. J. Appl. Physiol. 1985 (71), 2493.
Pramanick, S., Singodia, D., Chandel, V., 2013. Excipient selection in parenteral formulation development. Pharm. Times 45, 65–77.
Prestwich, G.D., 2008. Evaluating drug efficacy and toxicology in three dimensions: using synthetic extracellular matrices in drug discovery. Acc. Chem. Res. 41, 139–148.
Probst, M., Kühn, J.P., Scheuch, E., Seidlitz, A., Hadlich, S., Evert, K., Oswald, S., Siegmund, W., Weitschies, W., 2016. Simultaneous magnetic resonance imaging and pharmacokinetic analysis of intramuscular depots. J. Control. Release 227, 1–12.
Purslow, P.P., 2002. The structure and functional significance of variations in the connective tissue within muscle. Comp. Biochem. Physiol. A Mol. Integr. Physiol. 133, 947–966.
Roche, F., Sipilä, K., Honjo, S., Johansson, S., Tugues, S., Heino, J., Claesson-Welsh, L., 2015. Histidine-rich glycoprotein blocks collagen-binding integrins and adhesion of endothelial cells through low-affinity interaction with α2 integrin. Matrix Biol. 48, 89–99.
Romijn, R.A., Westein, E., Bouma, B., Schiphorst, M.E., Sixma, J.J., Lenting, P.J., Huizinga, E.G., 2003. Mapping the collagen-binding site in the von Willebrand factor-A3 domain. J. Biol. Chem. 278, 15035–15039.
Travis, J.A., Hughes, M.G., Wong, J.M., Wagner, W.D., Geary, R.L., 2001. Hyaluronan enhances contraction of collagen by smooth muscle cells and adventitial fibroblasts: Role of CD44 and implications for constrictive remodeling. Circ. Res. 88, 77–83.
Wassenaar, J.W., Boss, G.R., Christman, K.L., 2015. Decellularized skeletal muscle as an in vitro model for studying drug-extracellular matrix interactions. Biomaterials 64, 108–114.
Whyte, A., Parker, C., 2016. A review of the efficacy and tolerability of antipsychotic long-acting injections. Prog. Neurol. Psychiatry 20, 22–28.